Photonic band-gap effects on photoluminescence of silicon nanocrystals embedded in artificial opals

J. Valenta[a)]
Department of Chemical Physics and Optics, Charles University, Ke Karlovu 3, 121 16 Prague 2, Czech Republic

J. Linnros and R. Juhasz
Department of Microelectronics and Information Technology, Royal Institute of Technology, Electrum 229, 164 21 Kista-Stockholm, Sweden

J.-L. Rehspringer, F. Huber, and C. Hirlimann
Institut de Physique et Chimie des Matériaux de Strasbourg, GMI et GONLO, UMR46 CNRS-ULP-ECPM, 23, rue du Loess, F-67037 Strasbourg, France

S. Cheylan[b)] and R. G. Elliman
Electronic Materials Engineering Department, Research School of Physical Sciences and Engineering, Australian National University, Canberra, ACT 0200, Australia

(Received 3 September 2002; accepted 23 January 2003)

Si nanocrystals were formed in synthetic opals by Si-ion implantation and their optical properties studied using microphotoluminescence and reflection techniques. The properties of areas with high crystalline quality are compared with those of disordered regions of samples. The photoluminescence spectrum from Si nanocrystals embedded in silica spheres is narrowed by the inhibition of emission at wavelengths corresponding to the opal photonic pseudoband gap ($\sim$690 nm). Measurements of photoluminescence spectra from individual implanted silica spheres is also demonstrated and the number of emitting Si nanocrystals in single brightly emitting spheres is estimated to be of the order of one thousand. © *2003 American Institute of Physics.*
[DOI: 10.1063/1.1560565]

I. INTRODUCTION

Following the demonstration of strong room-temperature photoluminescence (PL) from electrochemically etched silicon many different light-emitting silicon nanostructures have been studied. In general, the quantum efficiency for silicon light emission increases significantly, by three to four orders of magnitude, in such low-dimensional structures.[1] This raises the possibility of all-silicon-based optoelectronics. However, the performance of Si-based light-emitting devices is still limited by a relatively low emission rate and broad emission spectrum. The inclusion of Si nanocrystals (NCs) into photonic structures provides an opportunity to manipulate the wavelength and direction of emission and, consequently, improve the functionality of such devices. In recent years, artificial opals have proven to be a reliable photonic structure for visible wavelengths.[2] Artificial opals are composed of submicrometer silica balls that are organized into a stochastic mixture of hexagonal-close-packed and face-centered-cubic (fcc) structure. However, such material has only optical stop bands (not a complete photonic band gap) due to the fact that the refraction index contrast between silica and voids (usually filled with air or some liquid) is insufficient. The central frequency of the stop bands depends on the direction of propagation through the opal crystal.[3] Several attempts to fill the opal voids with semiconductors —including silicon[4,5]—have been undertaken and their modified emission reported.[6–8] In contrast, the preparation of opals with semiconductor nanocrystals embedded inside the silica spheres is an alternative approach.[9,10]

The aim of this article is to report on the fabrication of Si NCs in artificial opals by means of Si-ion implantation and annealing. Using imaging microspectroscopy, we explore the modifications of Si-NC PL in opal structure and the emission of single silica balls containing Si NCs.

II. SAMPLE PREPARATION AND EXPERIMENTAL SETUP

Silica nanosphere suspensions were prepared following the modified Stöber–Finck process that has been shown to result in particle size dispersion of better than 2%. Large scale synthetic opals were prepared using electrosedimentation from colloidal solution. The sedimentation took approximately 4 days under static electric fields of 0.2 V/cm applied between a platinum grid and a mercury layer. Self-supporting opals were formed by partial sintering of the silica particles at 950 °C for 2 h. The mean diameter of the silica balls used in this study was about 300 nm [Fig. 1(a)]. Si NCs were formed inside the SiO_2 balls by Si^+ ion implantation (energy of 100 keV and dose of either 0.5 or $3\times10^{17}\,cm^{-2}$) and subsequent annealing at 1100 °C for 1 h in nitrogen. Figure 1 illustrates the structure of an opal sample imaged by a scan-

a)Author to whom correspondence should be addressed; electronic mail: jan.valenta@mff.cuni.cz
b)Present address: Instituto de Ciences Fotonicas ICFO, Jordi Girona 29, NEXUS II, 08034 Barcelona, Spain.

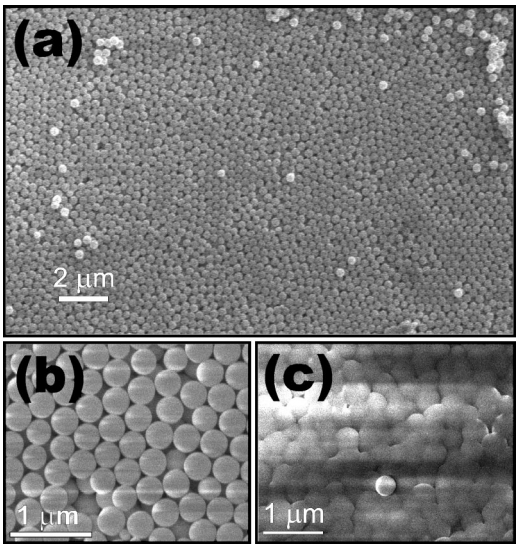

FIG. 1. Scanning electron micrographs of the synthetic opal structure (a). The magnified views in (b) and (c) show areas of opal implanted to fluences of 0.5 and 3×10^{17} cm^{-2}, respectively.

ning electron microscope. Figure 1(a) is a view of an unimplanted opal and highlights the presence of several isolated silica spheres accidentally removed from the bulk structure and lying on the surface. Figures 1(b) and 1(c) show details of structures implanted to low and high fluences, respectively. There are no apparent morphological modifications to the sample implanted to low dose but significant disturbances of the silica spheres are apparent after the high-dose irradiation. Similar deformation has previously been reported and has been used to controllably modify the shape of silica spheres.[11] A Transport of Ions in Matter TRIM calculation[12] of the implantation profile for 100 keV Si ions into quartz reveals a mean projected range of 150 nm. A simple numerical calculation gives an estimation of the redistribution of excess Si ions in the case of an opal structure (neglecting the curvature of the silica balls) showing that 66%, 29%, and 5% of the dose is stopped in the first, second, and third layer of silica spheres, respectively [implanting the (111) plane of a perfect opal fcc crystal].

PL and reflection spectra were measured using a microspectroscopy setup based on an imaging spectrograph connected to a conventional far-field microscope. A liquid-nitrogen-cooled charge coupled device camera was used for detection of images and spectra. The setup enables the measurement of a reflection or PL spectrum from any diffraction limited spot (i.e., roughly 500 nm for visible wavelengths). The UV line of a He–Cd laser (325 nm) was employed to excite the PL (in grazing incidence to the observed sample plane, excitation intensity up to 0.5 W/cm^2) and a halogen lamp light (focused and collected by the microscope objective lens) was used for reflection measurement. The experimental arrangement is schematically sketched in Fig. 2.

III. EXPERIMENTAL RESULTS AND DISCUSSION

Reflection microspectroscopy of opals reveals the presence of domains with various crystalline quality [Figs. 3(a) and 4(a)]. Sample regions with the best structure show a strong stop-band reflection in the red spectral region [Fig. 3(b)], while the areas with a disordered structure show much weaker reflection.

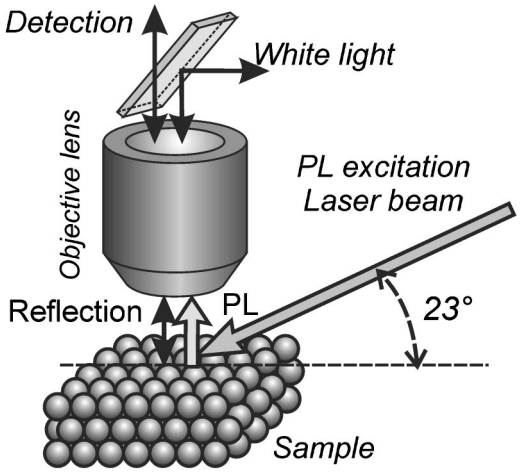

FIG. 2. Schematic diagram of the experimental arrangement employed to detect reflection and PL spectra from the same spot (with diameter down to the diffraction limit ~500 nm) of the opal crystal.

The stop band of unimplanted opal has a peak at 685 nm (1.807 eV). After implantation, the peak is slightly redshifted [to about 692 nm (1.79 eV)]. The corresponding theoretical value is given by:[13]

$$\lambda = 1.633\, d\, (n_a^2 - \sin^2\,\theta)^{1/2}, \tag{1}$$

where d is diameter of silica balls, n_a is average refractive index, and θ is the incident angle relative to the direction perpendicular to plane (111). According to Maxwell–Garnet model, the average refractive index is equal to

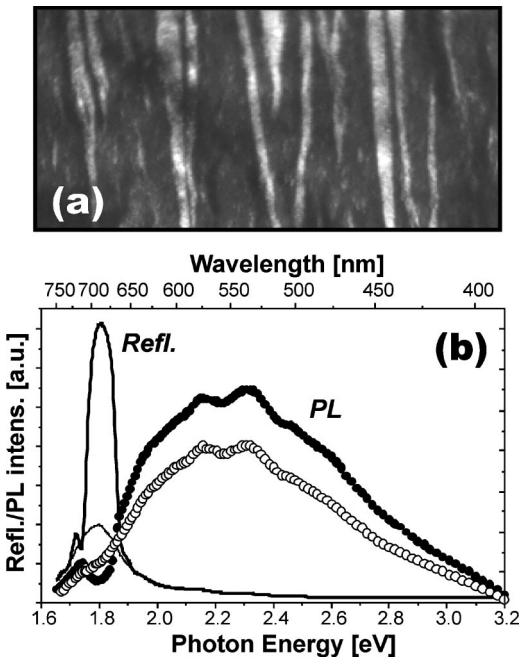

FIG. 3. (a) Reflection image of (0.79×0.37 mm) an unimplanted part of the opal surface. (b) Comparison of reflection (lines) and PL (dots) spectra from a highly reflective (bold line/black dots) and badly reflecting (narrow line/white dots) of an unimplanted opal.

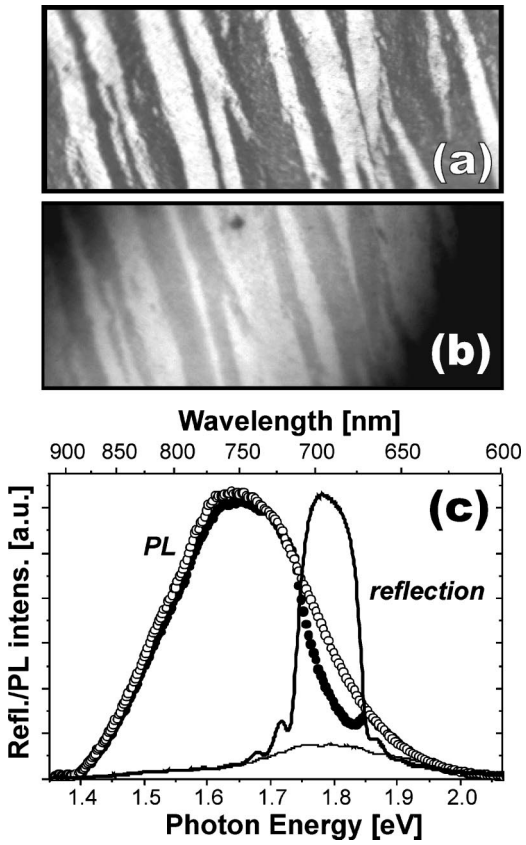

FIG. 4. Reflection image (a) and PL image (b) of the same area (1.13 $\times$0.54 mm) of moderately implanted opal crystal (contrast of the PL image is enhanced on purpose). (c) Comparison of reflection and PL spectra from highly reflecting (black dots) and badly reflecting (white dots) areas.

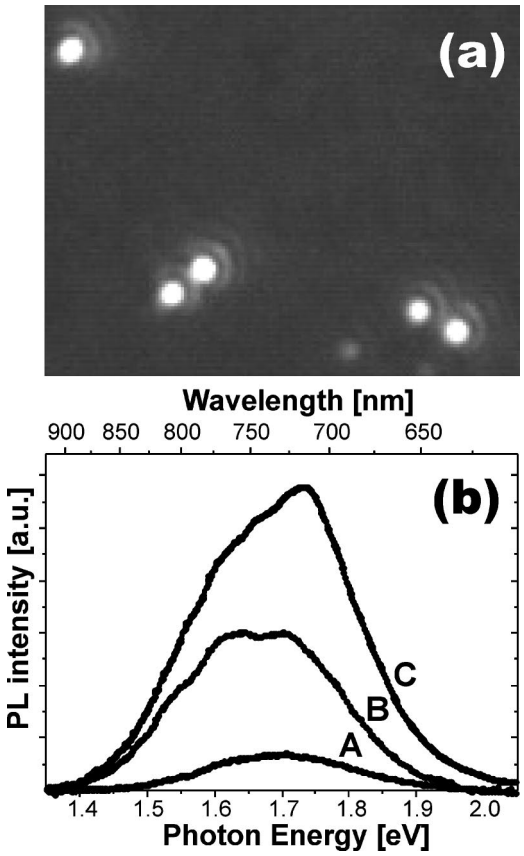

FIG. 5. (a) PL image (18$\times$18 μm) of a few strongly emitting silica spheres containing embedded Si NCs. (b) PL spectra from individual silica balls containing Si NCs.

$$n_a = [n_{\text{sphere}}^2 f + n_{\text{void}}^2 (1-f)]^{1/2}, \tag{2}$$

where f is a filling factor, which is theoretically 0.74. For silica spheres surrounded by air, we obtain $n_a = 1.35$. Considering balls with diameter of 310 nm, the stop band measured perpendicularly to plane (111) is expected to peak at 683 nm in good agreement with our observation. The presence of Si NCs in silica spheres induces only a small redshift of the stop band because the excess silicon concentration is restricted to a thin layer (at the peak of implantation profile the excess concentration of Si is estimated to be about 5.4 at. % for the low dose implant and 32 at. % for the high-dose implant).

Under UV-light excitation the nonimplanted regions show a weak blue-white PL emission [due to the oxygen-deficiency centers in silica, Fig. 3(b)][14] while implanted regions show strong red PL typical of Si NCs in SiO_2 [bluish emission being suppressed, Figs. 4(b) and 4(c)]. In places with excellent stop-band reflection, the PL emission is strongly reduced up to 50% of expected level within the spectral range of the stop band [compare PL spectra detected on ordered (black dots) and disordered (white dots) crystalline domains—Figs. 3(b) and 4(c).

Zhang and co-workers[9] have also studied ion-implanted opals but used relatively high implantation energy that probably caused significant distortion of the silica spheres (in a way similar to the case of our strongly implanted opal). They observed PL typical of Si NCs but no deep changes induced by the stop band. Our experiments give a clear demonstration of a strong trapping of PL from Si NCs (embedded in the silica spheres) by an opal metacrystal.

The application of a sensitive imaging spectroscope also enabled another interesting observation—the detection of PL from single implanted silica spheres. Because the opal is fragile, many silica spheres are removed (by the manipulation and transport of the sample) from their regular position in the crystal to other place on the opal surface [see Fig. 1(a)]. For implanted spheres close to the implant boundary, this can result in their relocation to the unimplanted surface. Such spheres then show up as strongly emitting spots on a surface with low background emission [see Fig. 5(a)]. Several such spheres were detected and their emission spectra measured using an imaging spectrograph [Fig. 5(b) shows three such spectra]. The PL intensity from these spheres was found to vary significantly presumably because they can originate from either the first or the second (or even third) implanted opal layer. In some cases, the broad PL spectral band appears to contain structure (Fig. 5, curves B and C) and it is interesting to speculate on the origin of such an effect. For spheres of diameter equal to (or greater than) half a wavelength of the Si NC PL emission (i.e., around 370 nm), this could arise from cavity resonances (whispering-gallery modes) associated with light trapping in the spheres.[15,16] If confirmed, this effect could provide another

means to manipulate emission from Si NCs. There are however other possible reasons for the observed spectral structures, e.g., fringes due to the photonic pseudogap, interference due to the presence of layers of different refraction index below the emitting sphere.

Finally, the number of light-emitting Si NCs in a single silica sphere can be estimated by comparing the total PL intensity of an implanted single sphere with that of a single emitting Si NC measured under the same experimental conditions.[17] The best total PL signal from a single Si NC was found to be about 36 counts/s under 0.5 W/cm^2 excitation by the 325 nm line of a continuous-wave (cw) laser. In comparison, the integrated PL signal for the best emitting silica spheres (e.g., Fig. 5, curve C) is around 35 000 counts/s. Therefore, the sphere should contain roughly one thousand efficiently emitting Si NCs. This gives only an order of magnitude estimate for the number of emitting Si NCs because many individual Si nanocrystals have lower emission intensity and effects due to nanocrystal interactions, silica sphere morphology, and chemical composition have been neglected.

We speculate that single efficiently emitting silica spheres with embedded Si NCs could potentially be used as efficient fluorescence tags in special cases. (We observe negligible bleaching of their emission under excitation by 325 nm line of a cw He–Cd laser with intensity up to 1 W/cm^2.)

IV. CONCLUSIONS

The results presented in this study demonstrate the possibility of forming photonic band-gap structures that incorporate Si nanocrystals. This was achieved by studying the PL emission and reflectivity of ion implanted synthetic opals composed of regular silica spheres of mean diameter 300 nm. The influence of the stop band on the PL emission from Si NCs was shown to be relatively strong even though the NCs are concentrated mainly in the first layer of silica spheres. Such (and more refined) structures have the potential to provide improved Si-based optoelectronic devices and structures.

ACKNOWLEDGMENTS

This work was supported by GACR (202/03/0789), NATO (PST.CLG.978100), and by the Royal Swedish Academy of Sciences. One of the authors (J.V.) appreciates financial support from the French government (program Echange).

[1] *Silicon-based Microphotonics: from Basics to Applications*, Proceeding of the E. Fermi Schools, Course CXLI, edited by O. Bisi, S. U. Campisano, L. Pavesi, and F. Priolo (IOS Press, Amsterdam, 1999).
[2] V. N. Bogomolov, S. V. Gaponenko, I. N. Germanenko, A. M. Kapitonov, E. P. Petrov, N. V. Gaponenko, A. V. Prokofjev, A. N. Ponyavina, N. I. Silvanovich, and S. M. Samoilovich, Phys. Rev. E **55**, 7619 (1997).
[3] Y. A. Vlasov, V. N. Astratov, O. Z. Karimov, A. A. Kalpyanskii, V. N. Bogomolov, and A. V. Prokofiev, Phys. Rev. B **55**, R13357 (1997).
[4] Y. A. Vlasov, X.-Z. Bo, J. C. Sturm, and D. J. Norris, Nature (London) **414**, 289 (2001).
[5] C. Díaz-Guerra, J. Piqueras, V. G. Golubev, D. A. Kurdyukov, and A. B. Pevtsov, J. Appl. Phys. **90**, 3659 (2001).
[6] S. V. Gaponenko, A. M. Kapitonov, V. N. Bogomolov, A. V. Prokofiev, A. Eychmüller, and A. L. Rogach, JETP Lett. **68**, 142 (1998).
[7] S. G. Romanov, A. V. Fokin, and R. M. De La Rue, Appl. Phys. Lett. **74**, 1821 (1999).
[8] Y. A. Vlasov, M. Deutch, and D. J. Norris, Appl. Phys. Lett. **76**, 1627 (2000).
[9] M. Ajgaonkar, Y. Zhang, H. Grebel, and C. W. White, Appl. Phys. Lett. **75**, 1532 (1999).
[10] Y. Zhang, S. Vijayalakshmi, M. Ajgaonkar, and H. Grebel, J. Opt. Soc. Am. B **17**, 1967 (2000).
[11] T. van Dillen, E. Snoeks, W. Fukarek, C. M. van Kats, K. P. Velikov, A. van Blaaderen, and A. Polman, Nucl. Instrum. Methods Phys. Res. B **175**, 350 (2001).
[12] The Stopping and Range of Ions in Solids, by J. F. Ziegler, J. P. Biersack, and U. Littmark (Pergamon, New York, 1996).
[13] Z. Z. Gu, Q. B. Meng, S. Hayami, A. Fujishima, and O. Sato, J. Appl. Phys. **90**, 2042 (2001), and references therein.
[14] L. Skuja, J. Non-Cryst. Solids **239**, 16 (1998).
[15] M. A. Kaliteevski, S. Brand, R. A. Abram, V. V. Nikolaev, M. V. Maximov, C. M. Sotomayor Torres, and A. V. Kavokin, Phys. Rev. B **64**, 115305 (2001).
[16] M. V. Artemyev and U. Woggon, Appl. Phys. Lett. **76**, 1353 (2000).
[17] J. Valenta, R. Juhasz, and J. Linnros, Appl. Phys. Lett. **80**, 1070 (2002).